Upper Limit for the Decay $B^- \to \tau^- \overline{\nu}\_\tau$ and Measurement of the $b \to \tau \overline{\nu}\_\tau X$ Branching Ratio

P. Abreu, W. Adam, T. Adye, P. Adzic, I. Ajinenko, Z. Albrecht, T. Alderweireld, G.D. Alekseev, R. Alemany, T. Allmendinger, et al.

EUROPEAN ORGANIZATION FOR NUCLEAR RESEARCH

CERN–EP/99–162

12 November 1999

Upper Limit for the Decay $B^- \to \tau^- \bar{\nu}_\tau$ and Measurement of the $b \to \tau \bar{\nu}_\tau X$ Branching Ratio

DELPHI Collaboration

Abstract

Using the data sample of hadronic Z^0 decays collected by the DELPHI experiment in the 1992-1995 LEP1 period, the leptonic decay of the charged B mesons ($B^- \to \tau^- \bar{\nu}_\tau$) has been studied. The analysis was done in both leptonic $\tau^- \to \ell^- \nu_\tau \bar{\nu}_\ell$ and hadronic $\tau^- \to \nu_\tau X$ decay channels. No excess was observed in data and the upper limit BR($B^- \to \tau^- \bar{\nu}_\tau$) $< 1.1 \times 10^{-3}$ at the 90% confidence level was obtained. This result is consistent with Standard Model expectations and puts a constraint on the ratio $\tan\beta/M_{H^\pm} < 0.45$ (GeV/c^2)$^{-1}$ in the framework of models with two Higgs doublets (any type II Higgs doublet model). From the missing energy distribution, the branching ratio of $b \to \tau \bar{\nu}_\tau X$ was measured in the hadronic channel $\tau \to \nu_\tau X'$. The result, BR($b \to \tau \bar{\nu}_\tau X$)= $(2.19 \pm 0.24\ (stat) \pm 0.40\ (syst))$%, is consistent with the Standard Model prediction and with previous experimental measurements.

(Submitted to Physics Letters B)

P.Abreu[22], W.Adam[52], T.Adye[38], P.Adzic[12], I.Ajinenko[44], Z.Albrecht[18], T.Alderweireld[2], G.D.Alekseev[17], R.Alemany[51], T.Allmendinger[18], P.P.Allport[23], S.Almehed[25], U.Amaldi[9,29], N.Amapane[47], S.Amato[49], E.G.Anassontzis[3], P.Andersson[46], A.Andreazza[9], S.Andringa[22], P.Antilogus[26], W-D.Apel[18], Y.Arnoud[9], B.Åsman[46], J-E.Augustin[26], A.Augustinus[9], P.Baillon[9], P.Bambade[20], F.Barao[22], G.Barbiellini[48], R.Barbier[26], D.Y.Bardin[17], G.Barker[18], A.Baroncelli[40], M.Battaglia[16], M.Baubillier[24], K-H.Becks[54], M.Begalli[6], A.Behrmann[54], P.Beilliere[8], Yu.Belokopytov[9], N.C.Benekos[33], A.C.Benvenuti[5], C.Berat[15], M.Berggren[24], D.Bertrand[2], M.Besancon[41], M.Bigi[47], M.S.Bilenky[17], M-A.Bizouard[20], D.Bloch[10], H.M.Blom[32], M.Bonesini[29], M.Boonekamp[41], P.S.L.Booth[23], A.W.Borgland[4], G.Borisov[20], C.Bosio[43], O.Botner[50], E.Boudinov[32], B.Bouquet[20], C.Bourdarios[20], T.J.V.Bowcock[23], I.Boyko[17], I.Bozovic[12], M.Bozzo[14], M.Bracko[45], P.Branchini[40], R.A.Brenner[50], P.Bruckman[9], J-M.Brunet[8], L.Bugge[34], T.Buran[34], B.Buschbeck[52], P.Buschmann[54], S.Cabrera[51], M.Caccia[28], M.Calvi[29], T.Camporesi[9], V.Canale[39], F.Carena[9], L.Carroll[23], C.Caso[14], M.V.Castillo Gimenez[51], A.Cattai[9], F.R.Cavallo[5], V.Chabaud[9], Ph.Charpentier[9], P.Checchia[37], G.A.Chelkov[17], R.Chierici[47], P.Chliapnikov[9,44], P.Chochula[7], V.Chorowicz[26], J.Chudoba[31], K.Cieslik[19], P.Collins[9], R.Contri[14], E.Cortina[51], G.Cosme[20], F.Cossutti[9], H.B.Crawley[1], D.Crennell[38], S.Crepe[15], G.Crosetti[14], J.Cuevas Maestro[35], S.Czellar[16], M.Davenport[9], W.Da Silva[24], G.Della Ricca[48], P.Delpierre[27], N.Demaria[9], A.De Angelis[48], W.De Boer[18], C.De Clercq[2], B.De Lotto[48], A.De Min[37], L.De Paula[49], H.Dijkstra[9], L.Di Ciaccio[9,39], J.Dolbeau[8], K.Doroba[53], M.Dracos[10], J.Drees[54], M.Dris[33], A.Duperrin[26], J-D.Durand[9], G.Eigen[4], T.Ekelof[50], G.Ekspong[46], M.Ellert[50], M.Elsing[9], J-P.Engel[10], M.Espirito Santo[9], G.Fanourakis[12], D.Fassouliotis[12], J.Fayot[24], M.Feindt[18], A.Ferrer[51], E.Ferrer-Ribas[20], F.Ferro[14], S.Fichet[24], A.Firestone[1], U.Flagmeyer[54], H.Foeth[9], E.Fokitis[33], F.Fontanelli[14], B.Franek[38], A.G.Frodesen[4], R.Fruhwirth[52], F.Fulda-Quenzer[20], J.Fuster[51], A.Galloni[23], D.Gamba[47], S.Gamblin[20], M.Gandelman[49], C.Garcia[51], C.Gaspar[9], M.Gaspar[49], U.Gasparini[37], Ph.Gavillet[9], E.N.Gazis[33], D.Gele[10], T.Geralis[12], L.Gerdyukov[44], N.Ghodbane[26], I.Gil[51], F.Glege[54], R.Gokieli[9,53], B.Golob[9,45], G.Gomez-Ceballos[42], P.Goncalves[22], I.Gonzalez Caballero[42], G.Gopal[38], L.Gorn[1], Yu.Gouz[44], V.Gracco[14], J.Grahl[1], E.Graziani[40], P.Gris[41], G.Grosdidier[20], K.Grzelak[53], J.Guy[38], C.Haag[18], F.Hahn[9], S.Hahn[54], S.Haider[9], A.Hallgren[50], K.Hamacher[54], J.Hansen[34], F.J.Harris[36], V.Hedberg[9,25], S.Heising[18], J.J.Hernandez[51], P.Herquet[2], H.Herr[9], T.L.Hessing[36], J.-M.Heuser[54], E.Higon[51], S-O.Holmgren[46], P.J.Holt[36], S.Hoorelbeke[2], M.Houlden[23], J.Hrubec[52], M.Huber[18], K.Huet[2], G.J.Hughes[23], K.Hultqvist[9,46], J.N.Jackson[23], R.Jacobsson[9], P.Jalocha[19], R.Janik[7], Ch.Jarlskog[25], G.Jarlskog[25], P.Jarry[41], B.Jean-Marie[20], D.Jeans[36], E.K.Johansson[46], P.Jonsson[26], C.Joram[9], P.Juillot[10], L.Jungermann[18], F.Kapusta[24], K.Karafasoulis[12], S.Katsanevas[26], E.C.Katsoufis[33], R.Keranen[18], G.Kernel[45], B.P.Kersevan[45], B.A.Khomenko[17], N.N.Khovanski[17], A.Kiiskinen[16], B.King[23], A.Kinvig[23], N.J.Kjaer[9], O.Klapp[54], H.Klein[9], P.Kluit[32], P.Kokkinias[12], V.Kostioukhine[44], C.Kourkoumelis[3], O.Kouznetsov[17], M.Krammer[52], E.Kriznic[45], J.Krstic[12], Z.Krumstein[17], P.Kubinec[7], J.Kurowska[53], K.Kurvinen[16], J.W.Lamsa[1], D.W.Lane[1], V.Lapin[44], J-P.Laugier[41], R.Lauhakangas[16], G.Leder[52], F.Ledroit[15], V.Lefebure[2], L.Leinonen[46], A.Leisos[12], R.Leitner[31], G.Lenzen[54], V.Lepeltier[20], T.Lesiak[19], M.Lethuillier[41], J.Libby[36], W.Liebig[54], D.Liko[9], A.Lipniacka[9,46], I.Lippi[37], B.Loerstad[25], J.G.Loken[36], J.H.Lopes[49], J.M.Lopez[42], R.Lopez-Fernandez[15], D.Loukas[12], P.Lutz[41], L.Lyons[36], J.MacNaughton[52], J.R.Mahon[6], A.Maio[22], A.Malek[54], T.G.M.Malmgren[46], S.Maltezos[33], V.Malychev[17], F.Mandl[52], J.Marco[42], R.Marco[42], B.Marechal[49], M.Margoni[37], J-C.Marin[9], C.Mariotti[9], A.Markou[12], C.Martinez-Rivero[20], F.Martinez-Vidal[51], S.Marti i Garcia[9], J.Masik[13], N.Mastroyiannopoulos[12], F.Matorras[42], C.Matteuzzi[29], G.Matthiae[39], F.Mazzucato[37], M.Mazzucato[37], M.Mc Cubbin[23], R.Mc Kay[1], R.Mc Nulty[23], G.Mc Pherson[23], C.Meroni[28], W.T.Meyer[1], A.Miagkov[44], E.Migliore[9], L.Mirabito[26], W.A.Mitaroff[52], U.Mjoernmark[25], T.Moa[46], M.Moch[18], R.Moeller[30], K.Moenig[9,11], M.R.Monge[14], D.Moraes[49], X.Moreau[24], P.Morettini[14], G.Morton[36], U.Mueller[54], K.Muenich[54], M.Mulders[32], C.Mulet-Marquis[15], R.Muresan[25], W.J.Murray[38], B.Muryn[19], G.Myatt[36], T.Myklebust[34], F.Naraghi[15], M.Nassiakou[12], F.L.Navarria[5], S.Navas[51], K.Nawrocki[53], P.Negri[29], N.Neufeld[9], R.Nicolaidou[41], B.S.Nielsen[30], P.Niezurawski[53], M.Nikolenko[10,17], V.Nomokonov[16], A.Nygren[25], V.Obraztsov[44], A.G.Olshevski[17], A.Onofre[22], R.Orava[16], G.Orazi[10], K.Osterberg[16], A.Ouraou[41], M.Paganoni[29], S.Paiano[5], R.Pain[24], R.Paiva[22], J.Palacios[36], H.Palka[19], Th.D.Papadopoulou[9,33], L.Pape[9], C.Parkes[9], F.Parodi[14], U.Parzefall[23], A.Passeri[40], O.Passon[54], T.Pavel[25], M.Pegoraro[37], L.Peralta[22], M.Pernicka[52], A.Perrotta[5], C.Petridou[48], A.Petrolini[14], H.T.Phillips[38], F.Pierre[41], M.Pimenta[22], E.Piotto[28], T.Podobnik[45], M.E.Pol[6], G.Polok[19], P.Poropat[48], V.Pozdniakov[17], P.Privitera[39], N.Pukhaeva[17], A.Pullia[29], D.Radojicic[36], S.Ragazzi[29], H.Rahmani[33], J.Rames[13], P.N.Ratoff[21], A.L.Read[34], P.Rebecchi[9], N.G.Redaelli[29], J.Rehn[18], D.Reid[32], R.Reinhardt[54], P.B.Renton[36], L.K.Resvanis[3], F.Richard[20], J.Ridky[13], G.Rinaudo[47], I.Ripp-Baudot[10], O.Rohne[34], A.Romero[47], P.Ronchese[37], E.I.Rosenberg[1], P.Rosinsky[7], P.Roudeau[20], T.Rovelli[5], Ch.Royon[41], V.Ruhlmann-Kleider[41], A.Ruiz[42], H.Saarikko[16], Y.Sacquin[41], A.Sadovsky[17], G.Sajot[15], J.Salt[51], D.Sampsonidis[12], M.Sannino[14], Ph.Schwemling[24], B.Schwering[54], U.Schwickerath[18], F.Scuri[48], P.Seager[21], Y.Sedykh[17], A.M.Segar[36], N.Seibert[18], R.Sekulin[38], R.C.Shellard[6], M.Siebel[54], L.Simard[41], F.Simonetto[37], A.N.Sisakian[17], G.Smadja[26], N.Smirnov[44], O.Smirnova[25], G.R.Smith[38], A.Sokolov[44], A.Sopczak[18], R.Sosnowski[53], T.Spassov[22], E.Spiriti[40], S.Squarcia[14], C.Stanescu[40], S.Stanic[45], M.Stanitzki[18], K.Stevenson[36], A.Stocchi[20], J.Strauss[52], R.Strub[10], B.Stugu[4], M.Szczekowski[53], M.Szeptycka[53], T.Tabarelli[29], A.Taffard[23], F.Tegenfeldt[50], F.Terranova[29], J.Thomas[36], J.Timmermans[32], N.Tinti[5], L.G.Tkatchev[17], M.Tobin[23], S.Todorova[9], A.Tomaradze[2], B.Tome[22], A.Tonazzo[9], L.Tortora[40], P.Tortosa[51], G.Transtromer[25], D.Treille[9], G.Tristram[8], M.Trochimczuk[53], C.Troncon[28],

M-L.Turluer[41], I.A.Tyapkin[17], P.Tyapkin[25], S.Tzamarias[12], O.Ullaland[9], V.Uvarov[44], G.Valenti[9,5], E.Vallazza[48], P.Van Dam[32], W.Van den Boeck[2], W.K.Van Doninck[2], J.Van Eldik[9,32], A.Van Lysebetten[2], N.van Remortel[2], I.Van Vulpen[32], G.Vegni[28], L.Ventura[37], W.Venus[38,9], F.Verbeure[2], P.Verdier[26], M.Verlato[37], L.S.Vertogradov[17], V.Verzi[28], D.Vilanova[41], L.Vitale[48], E.Vlasov[44], A.S.Vodopyanov[17], G.Voulgaris[3], V.Vrba[13], H.Wahlen[54], C.Walck[46], A.J.Washbrook[23], C.Weiser[9], D.Wicke[54], J.H.Wickens[2], G.R.Wilkinson[36], M.Winter[10], M.Witek[19], G.Wolf[9], J.Yi[1], O.Yushchenko[44], A.Zalewska[19], P.Zalewski[53], D.Zavrtanik[45], E.Zevgolatakos[12], N.I.Zimin[17,25], A.Zintchenko[17], Ph.Zoller[10], G.C.Zucchelli[46], G.Zumerle[37]

[1] Department of Physics and Astronomy, Iowa State University, Ames IA 50011-3160, USA
[2] Physics Department, Univ. Instelling Antwerpen, Universiteitsplein 1, B-2610 Antwerpen, Belgium
and IIHE, ULB-VUB, Pleinlaan 2, B-1050 Brussels, Belgium
and Faculté des Sciences, Univ. de l'Etat Mons, Av. Maistriau 19, B-7000 Mons, Belgium
[3] Physics Laboratory, University of Athens, Solonos Str. 104, GR-10680 Athens, Greece
[4] Department of Physics, University of Bergen, Allégaten 55, NO-5007 Bergen, Norway
[5] Dipartimento di Fisica, Università di Bologna and INFN, Via Irnerio 46, IT-40126 Bologna, Italy
[6] Centro Brasileiro de Pesquisas Físicas, rua Xavier Sigaud 150, BR-22290 Rio de Janeiro, Brazil
and Depto. de Física, Pont. Univ. Católica, C.P. 38071 BR-22453 Rio de Janeiro, Brazil
and Inst. de Física, Univ. Estadual do Rio de Janeiro, rua São Francisco Xavier 524, Rio de Janeiro, Brazil
[7] Comenius University, Faculty of Mathematics and Physics, Mlynska Dolina, SK-84215 Bratislava, Slovakia
[8] Collège de France, Lab. de Physique Corpusculaire, IN2P3-CNRS, FR-75231 Paris Cedex 05, France
[9] CERN, CH-1211 Geneva 23, Switzerland
[10] Institut de Recherches Subatomiques, IN2P3 - CNRS/ULP - BP20, FR-67037 Strasbourg Cedex, France
[11] Now at DESY-Zeuthen, Platanenallee 6, D-15735 Zeuthen, Germany
[12] Institute of Nuclear Physics, N.C.S.R. Demokritos, P.O. Box 60228, GR-15310 Athens, Greece
[13] FZU, Inst. of Phys. of the C.A.S. High Energy Physics Division, Na Slovance 2, CZ-180 40, Praha 8, Czech Republic
[14] Dipartimento di Fisica, Università di Genova and INFN, Via Dodecaneso 33, IT-16146 Genova, Italy
[15] Institut des Sciences Nucléaires, IN2P3-CNRS, Université de Grenoble 1, FR-38026 Grenoble Cedex, France
[16] Helsinki Institute of Physics, HIP, P.O. Box 9, FI-00014 Helsinki, Finland
[17] Joint Institute for Nuclear Research, Dubna, Head Post Office, P.O. Box 79, RU-101 000 Moscow, Russian Federation
[18] Institut für Experimentelle Kernphysik, Universität Karlsruhe, Postfach 6980, DE-76128 Karlsruhe, Germany
[19] Institute of Nuclear Physics and University of Mining and Metalurgy, Ul. Kawiory 26a, PL-30055 Krakow, Poland
[20] Université de Paris-Sud, Lab. de l'Accélérateur Linéaire, IN2P3-CNRS, Bât. 200, FR-91405 Orsay Cedex, France
[21] School of Physics and Chemistry, University of Lancaster, Lancaster LA1 4YB, UK
[22] LIP, IST, FCUL - Av. Elias Garcia, 14-1^{o}, PT-1000 Lisboa Codex, Portugal
[23] Department of Physics, University of Liverpool, P.O. Box 147, Liverpool L69 3BX, UK
[24] LPNHE, IN2P3-CNRS, Univ. Paris VI et VII, Tour 33 (RdC), 4 place Jussieu, FR-75252 Paris Cedex 05, France
[25] Department of Physics, University of Lund, Sölvegatan 14, SE-223 63 Lund, Sweden
[26] Université Claude Bernard de Lyon, IPNL, IN2P3-CNRS, FR-69622 Villeurbanne Cedex, France
[27] Univ. d'Aix - Marseille II - CPP, IN2P3-CNRS, FR-13288 Marseille Cedex 09, France
[28] Dipartimento di Fisica, Università di Milano and INFN-MILANO, Via Celoria 16, IT-20133 Milan, Italy
[29] Dipartimento di Fisica, Univ. di Milano-Bicocca and INFN-MILANO, Piazza delle Scienze 2, IT-20126 Milan, Italy
[30] Niels Bohr Institute, Blegdamsvej 17, DK-2100 Copenhagen Ø, Denmark
[31] IPNP of MFF, Charles Univ., Areal MFF, V Holesovickach 2, CZ-180 00, Praha 8, Czech Republic
[32] NIKHEF, Postbus 41882, NL-1009 DB Amsterdam, The Netherlands
[33] National Technical University, Physics Department, Zografou Campus, GR-15773 Athens, Greece
[34] Physics Department, University of Oslo, Blindern, NO-1000 Oslo 3, Norway
[35] Dpto. Fisica, Univ. Oviedo, Avda. Calvo Sotelo s/n, ES-33007 Oviedo, Spain
[36] Department of Physics, University of Oxford, Keble Road, Oxford OX1 3RH, UK
[37] Dipartimento di Fisica, Università di Padova and INFN, Via Marzolo 8, IT-35131 Padua, Italy
[38] Rutherford Appleton Laboratory, Chilton, Didcot OX11 OQX, UK
[39] Dipartimento di Fisica, Università di Roma II and INFN, Tor Vergata, IT-00173 Rome, Italy
[40] Dipartimento di Fisica, Università di Roma III and INFN, Via della Vasca Navale 84, IT-00146 Rome, Italy
[41] DAPNIA/Service de Physique des Particules, CEA-Saclay, FR-91191 Gif-sur-Yvette Cedex, France
[42] Instituto de Fisica de Cantabria (CSIC-UC), Avda. los Castros s/n, ES-39006 Santander, Spain
[43] Dipartimento di Fisica, Università degli Studi di Roma La Sapienza, Piazzale Aldo Moro 2, IT-00185 Rome, Italy
[44] Inst. for High Energy Physics, Serpukov P.O. Box 35, Protvino, (Moscow Region), Russian Federation
[45] J. Stefan Institute, Jamova 39, SI-1000 Ljubljana, Slovenia and Laboratory for Astroparticle Physics,
Nova Gorica Polytechnic, Kostanjeviska 16a, SI-5000 Nova Gorica, Slovenia,
and Department of Physics, University of Ljubljana, SI-1000 Ljubljana, Slovenia
[46] Fysikum, Stockholm University, Box 6730, SE-113 85 Stockholm, Sweden
[47] Dipartimento di Fisica Sperimentale, Università di Torino and INFN, Via P. Giuria 1, IT-10125 Turin, Italy
[48] Dipartimento di Fisica, Università di Trieste and INFN, Via A. Valerio 2, IT-34127 Trieste, Italy
and Istituto di Fisica, Università di Udine, IT-33100 Udine, Italy
[49] Univ. Federal do Rio de Janeiro, C.P. 68528 Cidade Univ., Ilha do Fundão BR-21945-970 Rio de Janeiro, Brazil
[50] Department of Radiation Sciences, University of Uppsala, P.O. Box 535, SE-751 21 Uppsala, Sweden
[51] IFIC, Valencia-CSIC, and D.F.A.M.N., U. de Valencia, Avda. Dr. Moliner 50, ES-46100 Burjassot (Valencia), Spain
[52] Institut für Hochenergiephysik, Österr. Akad. d. Wissensch., Nikolsdorfergasse 18, AT-1050 Vienna, Austria
[53] Inst. Nuclear Studies and University of Warsaw, Ul. Hoza 69, PL-00681 Warsaw, Poland
[54] Fachbereich Physik, University of Wuppertal, Postfach 100 127, DE-42097 Wuppertal, Germany

1 Introduction

The purely leptonic decay $B^- \to \tau^- \bar{\nu}_\tau$ is of particular interest to test for deviations from the Standard Model. In the Standard Model, the heavy b quark annihilates with the light $\bar{u}$ antiquark into a virtual W^- boson which decays leptonically. The width of the decay $B^- \to \tau^- \bar{\nu}_\tau$ [1] is thus predicted to be:

$$\Gamma^{SM}(B^- \to \tau^- \bar{\nu}_\tau) = \frac{G_F^2 f_B^2 |V_{ub}|^2}{8\pi} m_B^3 \left(\frac{m_\tau}{m_B}\right)^2 \left(1 - \frac{m_\tau^2}{m_B^2}\right)^2 \quad (1)$$

where G_F is the Fermi coupling constant, $|V_{ub}|$ is the CKM matrix element, f_B is the B decay constant, m_B and m_τ are the B meson and τ lepton masses, respectively. The expected branching ratio is

$$\mathrm{BR}^{SM}(B^- \to \tau^- \bar{\nu}_\tau) = 6 \times 10^{-5} \cdot (f_B/190\ \mathrm{MeV})^2 \cdot (|V_{ub}|/0.003)^2,$$

using the most commonly accepted values for f_B (190 MeV) and $|V_{ub}|$ (0.003) [1]. However, there is still a large uncertainty on $\mathrm{BR}^{SM}(B^- \to \tau^- \bar{\nu}_\tau)$, because f_B and $|V_{ub}|$ are poorly determined at present.

Because of helicity conservation, partial decay widths are proportional to the square of the lepton mass. Purely leptonic decays into electron or muon are thus expected to have very small branching fractions: $\mathrm{BR}^{SM}(B^- \to \mu^- \bar{\nu}_\mu) \simeq 3 \times 10^{-7}$ and $\mathrm{BR}^{SM}(B^- \to e^- \bar{\nu}_e) \simeq 6 \times 10^{-12}$. For this reason, these decays are far from being observed at LEP.

The partial decay width for the decay $B^- \to \tau^- \bar{\nu}_\tau$ is also sensitive to physics beyond the Standard Model. In models with two Higgs doublets (the so called Type II Higgs models) the decay width can be significantly changed due to the contribution of charged Higgs bosons. In such models the branching ratio becomes [2]:

$$\mathrm{BR}(B^- \to \tau^- \bar{\nu}_\tau) = \mathrm{BR}^{SM}(B^- \to \tau^- \bar{\nu}_\tau) \cdot \left[\left(\frac{m_{B^-}}{m_{H^\pm}}\right)^2 \tan^2\beta - 1\right]^2 \quad (2)$$

where $m_{H^\pm}$ is the charged Higgs boson mass and $\tan\beta$ is the ratio of the vacuum expectation values of the two Higgs doublets.

No evidence for an enhancement relative to the Standard Model prediction has been observed by previous experimental studies from CLEO [3], ALEPH [4] and L3 [5], providing a constraint on the parameters of supersymmetric models with two Higgs doublets. The best upper limit so far has been obtained by L3: $\mathrm{BR}(B^- \to \tau^- \bar{\nu}_\tau) < 5.7 \times 10^{-4}$ at the 90% confidence level.

At LEP1 energies, the production of B_c mesons decaying leptonically can give a substantial contribution to the $\tau\bar{\nu}_\tau$ final state, because the coupling of the virtual $W^\pm$ involves the CKM matrix element V_{cb} instead of V_{ub}. The B_c meson has recently been observed by the CDF collaboration [6]. Its measured mass and lifetime are in agreement with current expectations. Within an uncertainty of a factor two, the relative fraction of $\tau\bar{\nu}_\tau$ final states coming from B_c and B_u production is given by:

$$\frac{N_{B_c}}{N_{B_u}} = 1.2\ \frac{f(b \to B_c)}{10^{-3}} \quad (3)$$

where $f(b \to B_c)$, the inclusive probability that a b quark hadronizes into a B_c meson, is expected to vary between 0.02% and 0.1% [7].

[1] In this paper, unless explicitly stated otherwise, corresponding statements for charge conjugate states are always implied.

The decay $b \to \tau\bar{\nu}_\tau X$, where X stands for all the other particles produced, represents another test of the Standard Model. The Standard Model predicts a value for the $b \to \tau\bar{\nu}_\tau X$ branching fraction of $(2.30 \pm 0.25)\%$ in the framework of the Heavy Quark Effective Theory (HQET) [8,9]. The supersymmetric extension of the Standard Model, with two Higgs doublets, predicts an enhancement for the decay $b \to \tau\bar{\nu}_\tau X$ [10,11], as it can be mediated by H^- and W^- exchanges. Therefore, an experimental measurement of this branching fraction could constrain the ratio of $\tan\beta/m_{H^\pm}$. The decay $b \to \tau\bar{\nu}_\tau X$ is the phase space suppressed channel compared with the other semileptonic b decays. But the $b \to \tau\bar{\nu}_\tau X$ decay is more sensitive to the contribution from the $H^\pm$-mediated exchanges, because this contribution is proportional to $(m_{lepton}/m_{H^\pm})^2$. Previous experimental measurements of BR($b \to \tau\bar{\nu}_\tau X$) by ALEPH [4], L3 [12] and OPAL [13] collaborations have confirmed the validity of Standard Model theoretical predictions.

In this paper, an upper limit on the exclusive branching fraction of $B^- \to \tau^-\bar{\nu}_\tau$ and a measurement of the inclusive branching fraction of $b \to \tau\bar{\nu}_\tau X$ are presented.

2 Sample selection

The data have been collected with the DELPHI detector at LEP during the 1992-1995 LEP1 running period. About 3.5 million hadronic Z^0 events were collected at the centre-of-mass energy around 91.2 GeV. The DELPHI detector and its performance have been described in references [14,15].

The primary vertex of the e^+e^- interaction was reconstructed on an event-by-event basis from the charged particle tracks and using a beam spot constraint. In the 1994 and 1995 data, the position of the primary vertex was determined with a precision of about 40 μm in the horizontal direction, and about 10 μm in the vertical direction. For the 1992 and 1993 data, the uncertainties were larger by about 50%.

Only charged particle tracks with impact parameters smaller than 2 cm, both along the beam axis and in the plane transverse to it, were accepted.

Electron and muon identifications have been described in [15]. In both exclusive and inclusive analyses with τ hadronic decays, electrons and muons had to be rejected with the highest efficiency. Thus, electrons were identified by using a loose tagging procedure, which has an efficiency of 80% and a hadron misidentification probability of about 1.6%. Muons were identified by requiring at least one hit in the muon chambers (very loose tagging), corresponding to an identification efficiency of 96% and a hadron misidentification probability of about 5.4%. The momentum of the lepton was required to be greater than 2 GeV/c.

Tighter requirements have been imposed for lepton identification and selection in the exclusive analysis using τ leptonic decays. For electrons (muons), they have an efficiency of 45% (70%) and correspond to a hadron misidentification probability of 0.2% (0.45%).

A sample of about 7 million simulated $q\bar{q}$ events was generated using the JETSET Parton Shower program [16] with b and c quark fragmentation described according to the Peterson parameterization [17]. These events have been processed through a full simulation of the DELPHI detector. For the exclusive analysis, a dedicated sample of 10000 events with a B^- meson decaying into $\tau\bar{\nu}_\tau$ has been generated and passed through the same simulation chain.

The selection criteria which have been applied to real and simulated event samples, in both the inclusive and exclusive analyses, are listed below:

a) hadronic events were selected by requiring a multiplicity of charged particles larger than seven and a total energy of charged particles (assumed to be pions) greater than 15 GeV;
b) all subdetectors needed for the analysis had to be fully operational;
c) a two jet topology has been selected by requiring that the thrust of the event was greater than 0.85;
d) in order to assure an optimal energy containment and to match the acceptance of the vertex detector, only the barrel region of DELPHI was considered by requiring that the direction of the thrust axis with respect to the beam axis satisfied $0.1 < |\cos\theta_t| < 0.7$;
e) the probability, P_E, that all charged particle tracks in an event originate from a common primary vertex was used as a b-tagging variable [18]. $Z^0 \to b\bar{b}$ events were selected using a P_E value smaller than 0.01, which gave an efficiency of 72% and a purity of 75%, when applied to hadronic Z^0 decays.

Each selected event has been divided into two hemispheres using the plane perpendicular to the thrust axis. In each hemisphere the missing energy, E_{miss}, has been calculated from the expression:

$$E_{miss} = E_{beam} - E_{vis} + E_{corr}, \tag{4}$$

where E_{beam} is the beam energy; $E_{corr} = (M^2_{same} - M^2_{oppo})/(4E_{beam})$ is a correction based on 4-momentum conservation, which make use of the invariant mass of all reconstructed particles both in the considered, M_{same}, and in the opposite, M_{oppo}, hemispheres. Thus, the distribution for E_{corr} peaks around zero and has a standard deviation of 1.3 GeV. The visible energy, E_{vis} in the considered hemisphere is:

$$E_{vis} = E_{ch} + E_{\gamma} + E_{oth} + E_{HCAL}, \tag{5}$$

where, for each hemisphere, E_{ch}, E_{γ}, E_{oth}, E_{HCAL} are the energy sums of charged particles, neutral electromagnetic (photon and non-photon) showers and of neutral hadronic calorimeter showers in each hemisphere, respectively. In the energies computation, the pion mass was assumed for charged particles and the photon mass for neutral particles.

The selections described in the following sections have been chosen in order to optimize the statistical significance of the measured branching fractions.

3 Upper limit for the decay $B^- \to \tau^- \bar{\nu}_\tau$

The decay $B^- \to \tau^- \bar{\nu}_\tau$ has been studied using the two main one prong decay modes of the τ lepton:

1) the leptonic channel, with a branching fraction close to 35% [22], in which the τ^- decays into $\ell^- \nu_\tau \bar{\nu}_\ell$ where ℓ^- is either an electron or a muon,
2) the hadronic channel, with a 65% branching fraction, in which the τ^- decays into $h^- \nu_\tau X$, where h^- is a charged hadron and X are other hadrons (mostly π^0's).

3.1 The τ leptonic decay channel

In the leptonic channel, as explained in Section 2, a charged lepton ℓ (μ or e) was identified using tight selection criteria. The lepton was selected in the hemisphere with the larger missing energy. According to the simulation of events with a $B^- \to \tau^- \bar{\nu}_\tau$ decay followed by $\tau^- \to \ell^- \nu_\tau \bar{\nu}_\ell$, this condition is satisfied in 90% of these events.

The impact parameter of each track was computed as the shortest distance between the track and the reconstructed primary vertex in the plane transverse to the beam direction. It was defined as positive if the angle between the impact parameter direction and the direction of the jet to which the track belonged was smaller than 90° [15]. The impact parameter of the lepton was then required to be positive and four times larger than its measured error.

In the τ^- rest frame, due to helicity conservation, the ℓ^- is emitted preferentially in a direction opposite to the flight direction of the τ^-. As a consequence in the laboratory frame, the lepton energy distributions for the signal and the background are rather similar, as shown in Figure 1, and the lepton energy cannot be used as a discriminating variable (here and below the background events are hadronic Z^0 events to which the same selection criteria are applied).

It is possible to reduce the background originating from heavy flavour semileptonic decays substantially by using a constrained kinematic fit. This approach is based on the fact that a b-hadron takes a large fraction of the jet energy and only the charged lepton is the final detectable particle, while there are additional B decay products in the case of the background from semileptonic decays. For the signal, the energy and momentum of the B meson can be reconstructed from energy-momentum conservation applied to the whole event:

$$\overrightarrow{P_B} = -\sum_{i\neq\ell} \overrightarrow{P_i}, \;\; E_B = \sqrt{s} - \sum_{i\neq\ell} E_i \; . \tag{6}$$

The summation is performed over all detected particles in the event except the lepton ℓ, which is assumed to be a τ decay product. The energies of all reconstructed particles (E_i^{fit}) are then varied in the kinematic fit, in order to minimize their deviations relative to the experimentally measured values (E_i^{meas}):

$$\chi^2 = \sum_{i\neq\ell} \frac{(E_i^{fit} - E_i^{meas})^2}{\sigma^2_{E_i^{meas}}} \tag{7}$$

applying the constraint $E_B^2 - \overrightarrow{P_B}^2 = M_B^2$.

In order to reject the background, E_B was required to be greater than 37 GeV (see Figure 1). All tracks in the lepton hemisphere, except the lepton, were required to have an impact parameter at less than 3σ from the primary vertex (σ is the measured error of the impact parameter), and to have a momentum, P_{max}, smaller than 5 GeV/c. The multiplicity, $mult$, of charged particles in the considered hemisphere was required to be smaller than 6. Since the measured lepton originates from two successive leptonic decays, an isolation criteria was applied. The sum of the energies, E_{cone}, and the invariant mass of all particles, M_{cone}, inside a cone with half opening angle of 0.5 radian around the lepton direction was required to be smaller than 12 GeV and 3 GeV/c^2, respectively. The distribution of these quantities, for both signal and background events, together with the chosen cuts, are shown in Figure 1.

After having applied the selection criteria, 3 events remain in real data, while 5 are predicted by the $q\bar{q}$ simulation. These selection criteria give a background rejection factor of 7410 (with a relative error of ± 0.24), while the selection efficiency of $B^- \rightarrow \tau^-\bar{\nu}_\tau$ leptonic events is $(6.5 \pm 1.3)\%$. Both values are calculated with respect to the number of events after the kinematic fit.

3.2 The τ hadronic decay channel

In the hadronic channel, only hemispheres with no $e^{\pm}$ or $\mu^{\pm}$ have been selected. In order to achieve a high rejection against semileptonic decays, the selection criteria used for lepton identification have been loosened. The leading hadron, h, was defined as the charged particle with the highest momentum in its hemisphere and with an impact parameter relative to the primary vertex larger than 4σ. In order to reduce the background it was required that the energy, E_h, of the leading hadron was smaller than 10 GeV. Furthermore, the hadron h was selected in the hemisphere with the larger missing energy (this selection has an efficiency of 88% for the signal events). Since most of the hadronic decays are of the type $\tau^- \rightarrow \nu_\tau h^- n\pi^0$ (with $n \geq 1$), identified π^0's and γ's have been selected inside a cone of half-opening angle equal to 0.5 radian around the direction of h. The energy and momentum of the B meson have been reconstructed as:

$$\overrightarrow{P_B} = - \sum_{i \neq h;\pi^0,\gamma/cone} \overrightarrow{P_i} \ , \ E_B = \sqrt{s} - \sum_{i \neq h;\pi^0,\gamma/cone} E_i, \qquad (8)$$

where the summation is performed over all detected particles of the event, except the charged hadron h and possible π^0's and γ's detected inside the cone, which are assumed to be τ decay product candidates. By analogy with the leptonic channel, the energies of all reconstructed particles have been corrected after a fit with the constraint $E_B^2 - \overrightarrow{P_B}^2 = M_B^2$.

In order to reject the background, E_B was required to be greater than 37 GeV (see Figure 2). The other charged particles in the hemisphere were selected if their impact parameter relative to the primary vertex was smaller than 4σ and if they had a momentum smaller than 2 GeV/c. The total neutral energy in the cone was required to be smaller than 4 GeV, the total energy and the invariant mass of the system of particles located inside the cone were required to be smaller than 7 GeV and 2 GeV/c^2, respectively. The multiplicity of charged particles in the hemisphere was required to be smaller than eight (see Figure 2).

After having applied the selection criteria, 17 events remain in real data, 20 are predicted by the $q\bar{q}$ simulation. These selection criteria give a background rejection factor of 7440 (with a relative error of ± 0.15), while the selection efficiency of $B^- \rightarrow \tau^- \bar{\nu}_\tau$ leptonic events is $(3.2 \pm 0.5)\%$. Both values are calculated with respect to the number of events after the kinematic fit.

3.3 Result

After having applied the selection criteria to both hadronic and leptonic channels, there is no evidence for an excess of events in data over the background estimate. Using the Bayesian approach for the combination of two channels with background [20], the number of events originating from $B^- \rightarrow \tau^- \bar{\nu}_\tau$ hadronic decays is found to be smaller than 3.5 at the 90% confidence level. The main sources of systematic errors have been included in the limit evaluation. They concern uncertainties affecting the b-tagging efficiency, the $\tau^- \rightarrow \ell^- \nu_\tau \bar{\nu_\ell}$ and $\tau^- \rightarrow \nu_\tau X$ branching ratios, the rate for lepton efficiency and hadron misidentification. The largest systematic error comes from the evaluation of the probability for b quarks to hadronize into charged B^- mesons, which is $0.397^{+0.018}_{-0.022}$ [22]. However, the contribution of the systematic errors to the upper limit turns out to be not significant. The upper limit on the number of events translates to:

$$\mathrm{BR}(B^- \rightarrow \tau^- \bar{\nu}_\tau) < 1.1 \times 10^{-3}$$

at the 90% confidence level.

4 Measurement of the $b \to \tau\bar{\nu}_\tau X$ branching ratio

The main signature of the $b \to \tau\bar{\nu}_\tau X$, $\tau \to \nu_\tau X'$ decay chain is a large missing energy originating from the production of two or three neutrinos. The main backgrounds are the semileptonic c decays and the semileptonic b decays into e or μ giving high-energy neutrinos. Another important background source consists of hadronic events with large missing energy due to the finite resolution of the detector and to the fact that there are regions where the detection efficiency is poor. To reduce these backgrounds, an enriched sample of $b \to \tau\bar{\nu}_\tau X$ candidates has been selected in two steps. First, as already mentioned, a sample of $Z^0 \to b\bar{b}$ events has been obtained by the selection criteria $P_E < 0.01$. Then, events have been retained if they have a large missing energy and no electron or muon candidate. In order to achieve a high rejection against heavy flavour semileptonic decays, leptons were identified with the loose criterion for electrons and the very loose criterion for muons. Hemispheres with such a lepton were rejected, which implies that the τ lepton had to decay through an hadronic channel $\tau \to \nu_\tau X'$, where X' are hadrons. Since this inclusive analysis is more sensitive to detector inefficiencies than the exclusive one, the criterion d) of Section 2 on the thrust axis polar direction was tightened by requiring: $0.2 < |\cos\theta_t| < 0.6$.

4.1 Energy correction procedure

In order to improve the agreement of the energy measurement between real data (RD_b) and simulation (MC_b), the following correction procedure has been used. The visible energy, E_{vis}, was corrected in a simulated sample enriched with light quark pair ($u\bar{u}$, $d\bar{d}$, $s\bar{s}$) events. Then the same correction was applied to the MC_b sample.

To obtain an enriched sample of light quark events in real data (RD_{uds}) and simulation (MC_{uds}), the selection criteria mentioned in Section 2 were used, except the criterion e) which was replaced by the condition e′) defined as:

e′) $0.6 < P_E < 1.0$, which corresponds to an efficiency of 41% and a purity of 91% for light quark pair events.

With this selection, the visible energy in the simulated sample, already defined in Section 2, has been parameterized as:

$$E_{vis}^{MC} = c_0 + c_1 \cdot E_{ch} + c_2 \cdot E_\gamma + c_3 \cdot E_{oth} + c_4 \cdot E_{HCAL}, \tag{9}$$

where the coefficients c_j $(j = 0 - 4)$ depend on the multiplicity of charged particles in the considered hemisphere.

The evaluation of these coefficients was performed by minimizing the sum:

$$\chi^2 = \sum_{k=1}^{5} \frac{(M_k^{RD_{uds}} - M_k^{MC_{uds}})^2}{D_k^{RD_{uds}}} \tag{10}$$

for each charged multiplicity in the hemisphere. In this expression, $M_1^{RD_{uds}}$ and $M_1^{MC_{uds}}$ are the mean visible energies in real data and simulated events, $M_k^{RD_{uds}}$ and $M_k^{MC_{uds}}$ $(k = 2, ..., 5)$ are central moments of order k of the E_{vis} distribution in real data and simulated events, respectively, and $D_k^{RD_{uds}}$ is the variance of the $M_k^{RD_{uds}}$ distribution. After having applied this correction to E_{vis} in the simulation sample, a good agreement has been obtained between the E_{miss} distributions in real and simulated events (Figure 3).

The same coefficients c_j have then been applied to the MC_b sample and a corrected value E_{vis}^{MC} has been obtained.

4.2 Result

A sub-sample of $b \to \tau\bar{\nu}_\tau X$ events, MC_b^τ, has been isolated from the simulated sample MC_b by requiring that the Z^0 decays into a $b\bar{b}$ pair and that the b decay products contain a τ lepton in one hemisphere. The complementary sub-sample, MC_b^{bkg}, contains all other possible decay modes and corresponds to the background simulation; it was subdivided into the semileptonic background, $MC_b^{\ell X}$, and the residual background, $MC_b^{res.bkg}$. Figure 4 shows the hemisphere missing energy distributions of the RD_b sample which was fitted as described in the following. The normalisation of the $MC_b^{\ell X}$ sample was fixed according to the known branching fractions and the estimated selection efficiencies (see Section 4.3). The normalisations of the MC_b^τ and $MC_b^{res.bkg}$ samples were treated as free parameters. The overall $MC_b^\tau + MC_b^{bkg}$ sample was normalized to the same number of events as in the RD_b sample.

Using the fitting procedure in the missing energy range from -5 GeV to 30 GeV, where the main part of the signal is concentrated, the branching fraction of $b \to \tau\bar{\nu}_\tau X$ is measured to be:

$$\mathrm{BR}(b \to \tau\bar{\nu}_\tau X) = (2.19 \pm 0.24\ (stat))\% \ .$$

Varying the chosen missing energy range by ± 5 GeV changes the observed branching fraction by $\pm 0.15\%$.

Figure 5 shows the difference between the distributions of events in the RD_b and MC_b^{bkg} sample. Its shape is consistent with that expected from the MC_b^τ component (shaded area).

4.3 Evaluation of systematic errors

The main physics background comes from the semileptonic decays of b and c quarks into e and μ. The uncertainty on the branching fractions of these decays contribute to the systematic error. Using the value $\mathrm{BR}(b \to \ell) = (10.99 \pm 0.23)\%$ [22] and varying this branching ratio by one standard deviation, an error on $\mathrm{BR}(b \to \tau\bar{\nu}_\tau X\ )$ of $\pm 0.004\%$ is obtained. In a similar way, the effect from the uncertainty on the cascade semileptonic branching fraction $\mathrm{BR}(b \to c \to \overline{\ell}) = (7.8 \pm 0.6)\%$ [22], has been evaluated to be $\pm 0.067\%$. From the uncertainty on the cascade semileptonic branching fraction, $\mathrm{BR}(b \to \overline{c} \to \ell) = (1.6 \pm 0.4)\%$ [23], a systematic error of $\pm 0.041\%$ is obtained. The effect from the uncertainty on the semileptonic branching fraction $\mathrm{BR}(c \to \overline{\ell}) = (9.6 \pm 0.5)\%$ [24], has been evaluated to be $\pm 0.035\%$.

The main part of the residual background from the semileptonic decays of b and c quarks is due to leptons with momenta smaller than 2 GeV/c. The uncertainty on the modelling of the leptonic decays, and consequently on the fractions of leptons with momenta smaller than 2 GeV/c (see Table 7 of reference [24]), contributes to a systematic uncertainty on the branching ratio which is evaluated to be $\pm 0.039\%$.

The only significant background involving τ leptons comes from the decay $D_s \to \tau\bar{\nu}_\tau$. Using the value of $(7 \pm 4)\%$ [22] and changing the branching ratio by one standard deviation, an error on $\mathrm{BR}(b \to \tau\bar{\nu}_\tau X\ )$ of $\pm 0.068\%$ is inferred. From an uncertainty on the $\mathrm{BR}(b \to D_s) = (18 \pm 5)\%$ [22], a systematic error on the branching ratio of $\pm 0.037\%$ is obtained.

For $b\overline{b}$ events, the missing energy spectrum depends on the mean energy of the decaying b-hadrons. Using the value of $\langle x_b \rangle = 0.702 \pm 0.008$ [23], the fragmentation distribution is changed in the simulation so that the mean value varies by $\pm 1\sigma$. Repeating the analysis

with the new fragmentation function, a systematic uncertainty of $\pm 0.21\%$ is obtained. Similarly the error from the value of $\langle x_c \rangle = 0.484 \pm 0.008$ [23] is found to be $\pm 0.03\%$.

A possible difference between data and simulation on the lepton identification has also to be taken into account. From an uncertainty of $\pm 1.2\%$ ($\pm 3\%$) on the μ (e) identification efficiency [15], a systematic error of $\pm 0.012\%$ ($\pm 0.025\%$) is obtained. Similarly, the uncertainties on the hadron misidentification, $\pm 2\%$ ($\pm 0.3\%$) for μ (e) [15], yield a systematic error on the branching ratio of $\pm 0.098\%$ ($\pm 0.012\%$).

The difference in the b-tagging purity for data and simulation is reflected in the systematic error, since the percentage of real $b\bar{b}$ events in the selected samples influences directly the value of the measured branching ratio. Having estimated this difference to be of the order of $\pm 2\%$, this gives a systematic error of $\pm 0.039\%$.

The variation of the branching fraction BR($b \to \tau \bar{\nu}_\tau X$) measured for different intervals of E_{miss} gives a systematic error of $\pm 0.15\%$.

Table 1 summarizes the systematic uncertainties on the measured branching fraction, calculated by changing the parameters described above by one standard deviation. The shape systematics accounts for the sensitivity of this measurement to the calibration of the shape of the missing energy distribution using a sample of events enriched in Z^0 decays into light quark pairs. Choosing different ways to tune the light quark simulation sample, the maximum spread (0.25%) in the variation of the extracted branching ratio has been used as a systematic uncertainty.

Combining all systematic contributions in quadrature, a total systematic error of $\pm 0.40\%$ is obtained.

Absolute variations of the parameters	$\Delta(b \to \tau \bar{\nu}_\tau X)$ (%)
BR($b \to \ell$) = $(10.99 \pm 0.23)\%$	0.004
BR($b \to$ c $\to \bar{\ell}$) = $(7.8 \pm 0.6)\%$	0.067
BR($b \to \bar{c} \to \ell$) = $(1.6 \pm 0.4)\%$	0.041
BR($c \to \bar{\ell}$) = $(9.6 \pm 0.5)\%$	0.035
$b, c \to \ell$ (or $\bar{\ell}$) decay models	0.039
BR($b \to D_s$) = $(18 \pm 5)\%$	0.037
BR($D_s \to \tau\nu$) = $(7 \pm 4)\%$	0.068
$<$ x$_b$ $>= 0.702 \pm 0.008$	0.210
$<$ x$_c$ $>= 0.484 \pm 0.008$	0.030
μ ID efficiency ($\pm 1.2\%$)	0.012
e ID efficiency ($\pm 3\%$)	0.025
hadron/μ misidentification ($\pm 2.0\%$)	0.098
hadron/e misidentification ($\pm 0.3\%$)	0.012
b-tagging purity ($\pm 2\%$)	0.039
E_{miss} range	0.150
shape	0.250
Total Systematic Error	0.396

Table 1: Systematic uncertainties on BR($b \to \tau \bar{\nu}_\tau X$)

5 Constraints on supersymmetric models

No indication of an enhancement of the $B^- \to \tau^- \bar{\nu}_\tau$ branching ratio has been observed when compared to the Standard Model prediction (BR^{SM}). In the Type II Higgs models,

the branching ratio $\mathrm{BR}(B^- \to \tau^- \bar{\nu}_\tau)$ is enhanced by a factor of $\left[\left(\frac{m_{B^-}}{m_{H^\pm}}\right)^2 \tan^2\beta - 1\right]^2$ [21]. Using the value of $m_{B^-} = 5279$ MeV/c^2 [22], and $\mathrm{BR}^{SM} = 6 \times 10^{-5}$ the following limit is obtained:

$$\frac{\tan\beta}{M_{H\pm}} < 0.46\ (\mathrm{GeV}/c^2)^{-1}$$

at the 90% confidence level.

Using the B_c contribution hypothesis [7], the branching ratio is modified to $\mathrm{BR}^{SM}(B_u + B_c) = \alpha \cdot \mathrm{BR}^{SM}(B_u)$, where α is a factor ranging from 1.24 to 2.2, which takes into account the $B_c \to \tau\bar{\nu}_\tau$ contribution. Using the lower bound for α, the previous limit becomes $\frac{\tan\beta}{M_{H\pm}} < 0.42\ (\mathrm{GeV}/c^2)^{-1}$ at the 90% confidence level.

No indication of a large enhancement of the branching ratio of $b \to \tau\bar{\nu}_\tau X$ has been found when compared to the Standard Model prediction. Using HQET and including one loop QCD corrections [21], the inclusive measurement of $b \to \tau\bar{\nu}_\tau X$ translates into a constraint on the charged Higgs mass in the framework of any Type II Higgs doublet model:

$$\frac{\tan\beta}{M_{H\pm}} < 0.45\ (\mathrm{GeV}/c^2)^{-1}$$

at the 90% confidence level.

6 Summary and conclusion

Using 3.5 million hadronic Z^0 decays collected in the 1992-1995 LEP1 period, the purely leptonic decay $B^- \to \tau^- \bar{\nu}_\tau$ has been studied in both the leptonic $\tau^- \to \ell^- \nu_\tau \bar{\nu}_\ell$ and hadronic $\tau^- \to \nu_\tau X$ decay channels. No signal has been observed, which corresponds to the following upper limit:

$$\mathrm{BR}(B^- \to \tau^- \bar{\nu}_\tau) < 1.1 \times 10^{-3} \text{ at the } 90\%\ C.L.$$

This limit is consistent with the Standard Model expectation $\mathrm{BR}^{SM} = 6 \times 10^{-5}$ and is competitive with respect to previous experimental results [3–5]. Since the branching ratio of $B^- \to \tau^- \bar{\nu}_\tau$ is expected to be significantly larger in models with two Higgs doublets, the following constraint is obtained in the framework of any Type II Higgs doublet model:

$$\frac{\tan\beta}{M_{H\pm}} < 0.46\ (\mathrm{GeV}/c^2)^{-1} \text{ at the } 90\%\ C.L.$$

This limit becomes slightly more stringent, if one includes the possible B_c contribution to the $\tau\bar{\nu}_\tau$ final state.

Using the observed missing energy distribution in a sample enriched in $b\bar{b}$ events but depleted in their semileptonic decays, the branching ratio:

$$\mathrm{BR}(b \to \tau\bar{\nu}_\tau X) = (2.19 \pm 0.24\ (stat) \pm 0.40\ (syst))\%$$

has been measured. This value is in agreement with the Standard Model prediction of $(2.30 \pm 0.25)\%$ [8] and with previous measurements by LEP experiments $(2.6 \pm 0.4)\%$ [22] (Figure 6). From this value a limit on

$$\frac{\tan\beta}{M_{H\pm}} < 0.45\ (\mathrm{GeV}/c^2)^{-1} \text{ at the } 90\%\ C.L.$$

has been obtained which is similar to the one deduced from the search for the exclusive channel $B^- \to \tau^- \bar{\nu}_\tau$ and is not influenced by the large uncertainty on f_B and $|V_{ub}|$. The upper limits for both inclusive and exclusive analysis are shown in Figure 7 together with the constraints derived from the direct search of charged Higgs boson at LEP ($M_{H^\pm} > 69$ GeV/c^2 [25]) and the measurements of $b \to s\gamma$ [26]. The dotted line shows how the limit could improve using the B_c contribution hypothesis.

Acknowledgments

We thank Y. Grossman of Stanford Linear Accelerator Center, for helping us to calculate the upper limit on $\tan\beta/M_{H\pm}$ and S. Slabospitsky of Protvino for useful discussion on B_c contamination.
We are greatly indebted to our technical collaborators, to the members of the CERN-SL Division for the excellent performance of the LEP collider, and to the funding agencies for their support in building and operating the DELPHI detector.
We acknowledge in particular the support of
Austrian Federal Ministry of Science and Traffics, GZ 616.364/2-III/2a/98,
FNRS–FWO, Belgium,
FINEP, CNPq, CAPES, FUJB and FAPERJ, Brazil,
Czech Ministry of Industry and Trade, GA CR 202/96/0450 and GA AVCR A1010521,
Danish Natural Research Council,
Commission of the European Communities (DG XII),
Direction des Sciences de la Matière, CEA, France,
Bundesministerium für Bildung, Wissenschaft, Forschung und Technologie, Germany,
General Secretariat for Research and Technology, Greece,
National Science Foundation (NWO) and Foundation for Research on Matter (FOM), The Netherlands,
Norwegian Research Council,
State Committee for Scientific Research, Poland, 2P03B06015, 2P03B1116 and SPUB/P03/178/98,
JNICT–Junta Nacional de Investigação Científica e Tecnológica, Portugal,
Vedecka grantova agentura MS SR, Slovakia, Nr. 95/5195/134,
Ministry of Science and Technology of the Republic of Slovenia,
CICYT, Spain, AEN96–1661 and AEN96-1681,
The Swedish Natural Science Research Council,
Particle Physics and Astronomy Research Council, UK,
Department of Energy, USA, DE–FG02–94ER40817.

References

[1] J. Alexander *et al.*, CLEO Collaboration, Phys. Rev. Lett. **77** (1996) 5000.
[2] W.-S. Hou, Phys. Rev. **D48** (1993) 2342.
[3] M. Artuso *et al.*, CLEO Collaboration, Phys. Rev. Lett. **75** (1995) 785.
[4] D. Buskulic *et al.*, ALEPH Collaboration, Phys. Lett. **B343** (1995) 444.
[5] M. Acciarri *et al.*, L3 Collaboration, Phys. Lett. **B396** (1997) 327.
[6] F. Abe *et al.*, CDF Collaboration, Phys. Rev. Lett. **81** (1998) 2432.
[7] M.L. Mangano and S.R. Slabospitsky, Phys. Lett. **B410** (1997) 299.
[8] A. Falk, Z. Ligeti, M. Neubert, Y. Nir, Phys. Lett. **B326** (1994) 145.
[9] P. Heiliger and L.M. Seghal, Phys. Lett. **B229** (1989) 409.
[10] B. Grzadkowski and W.-S. Hou, Phys. Lett. **B283** (1992) 427.
[11] G. Isidori, Phys. Lett. **B298** (1993) 409.
[12] M. Acciarri *et al.*, L3 Collaboration, Phys. Lett. **B332** (1994) 201.
[13] OPAL Collaboration, "Measurement of the Branching Ratios $b \to \tau^- \bar{\nu}_\tau X$ and $b \to D^{*+} \tau^- \bar{\nu}_\tau (X)$", submitted to the 1996 Warsaw ICHEP Conference, pa05-038.
[14] P. Aarnio *et al.*, DELPHI Collaboration, Nucl. Inst. Meth. **A303** (1991) 233.
[15] P. Abreu *et al.*, DELPHI Collaboration, Nucl. Inst. Meth. **A378** (1996) 57.
[16] T. Sjöstrand, Comp. Phys. Comm. **82** (1994) 74.
[17] C. Peterson *et al.*, Phys. Rev. **D27** (1983) 105.
[18] P. Abreu *et al.*, DELPHI Collaboration, Z. Phys. **C66** (1995) 323.
[19] S. Brandt *et al.*, Phys. Lett. **12** (1964) 57.
[20] V.F. Obraztsov, "Upper Limits Calculation", DELPHI Note 91-36 PHYS 94 (June 1991).
[21] Y. Grossman, H.E. Haber and Y. Nir, Phys. Lett. **B357** (1995) 630;
Y. Grossman and Z. Ligeti, Phys. Lett. **B332** (1994) 373.
[22] Review of Particle Physics, Eur. Phys. J. **C3** (1998) 1.
[23] The LEP Heavy Flavour Working Group, "Input Parameters for the LEP/SLD Electroweak Heavy Flavour Results for Summer 1998 Conferences", LEPHF/98-01, http://www.cern.ch/LEPEWWG/heavy/lephf9801.ps.gz .
[24] P. Abreu *et al.*, DELPHI Collaboration, "Determination of $P(c \to D^{*+})$ and $BR(c \to \ell^+)$ at LEP 1", preprint CERN-EP/99-67 (May 1999), submitted to Eur. Phys. J. C.
[25] The LEP working group for Higgs boson searches, "Limits on Higgs boson masses from combining the data of the four LEP experiments at $\sqrt{s}$ $\leq$183 GeV", preprint CERN-EP/99-060 (April 1999).
[26] M.S. Alam *et al.*, CLEO Collaboration, Phys. Rev. Lett. **74** (1995) 2885;
R. Barate *et al.*, ALEPH Collaboration, Phys. Lett. **B429** (1998) 169.

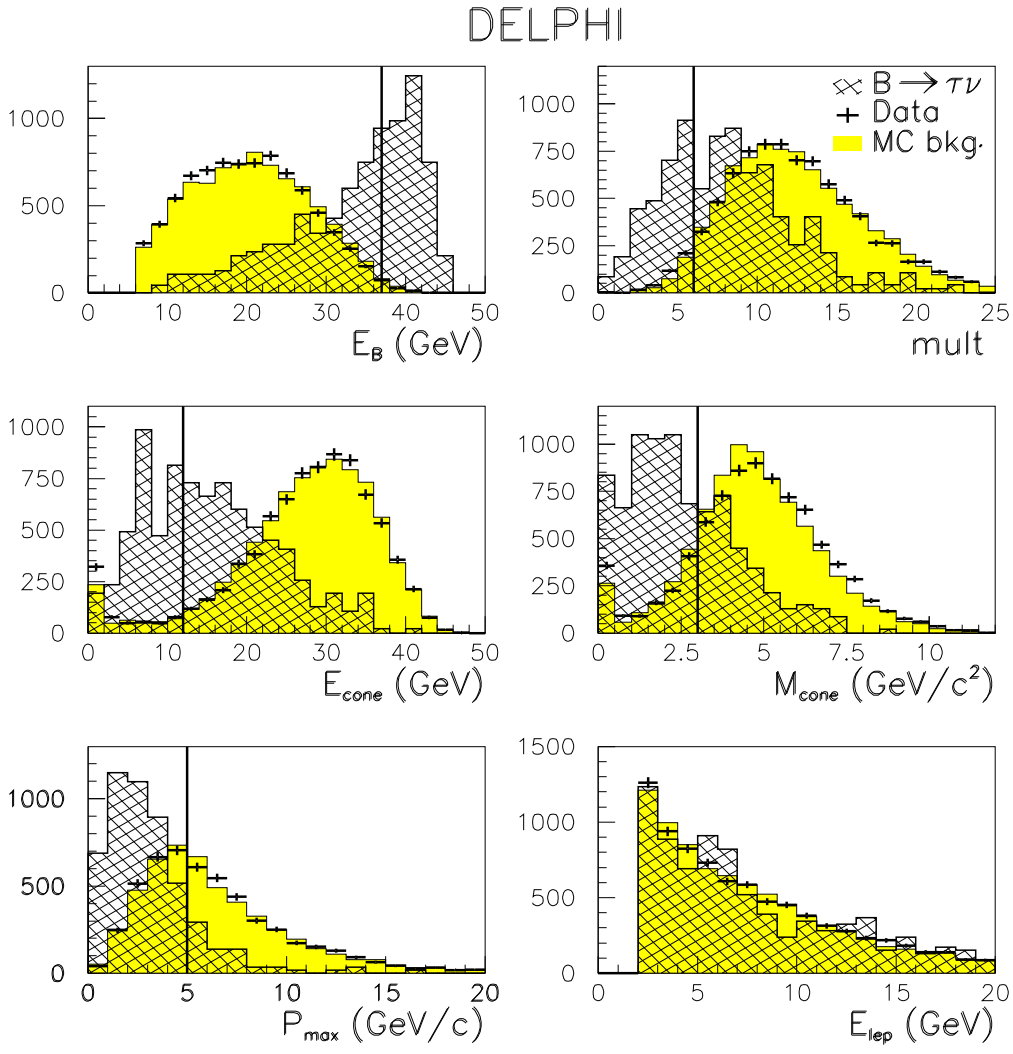

Figure 1: For the leptonic decay channel of the τ, simulated $B^- \to \tau^- \bar{\nu}_\tau$ signal (hatched) and background (shaded) distributions of the B meson energy, the hemisphere charged particle multiplicity, the total energy of particles inside the cone, the invariant mass of particles inside the cone, the maximum momentum of primary particles and the lepton energy (see Section 3.1). Measured distributions in data (crosses) have been superimposed after having normalized the distributions from the simulation to the same integrated luminosity. Distributions for signal events have been normalized, in an arbitrary way, to the same number of events in the histogram. The vertical line defines the values of the cuts (see Section 3.1).

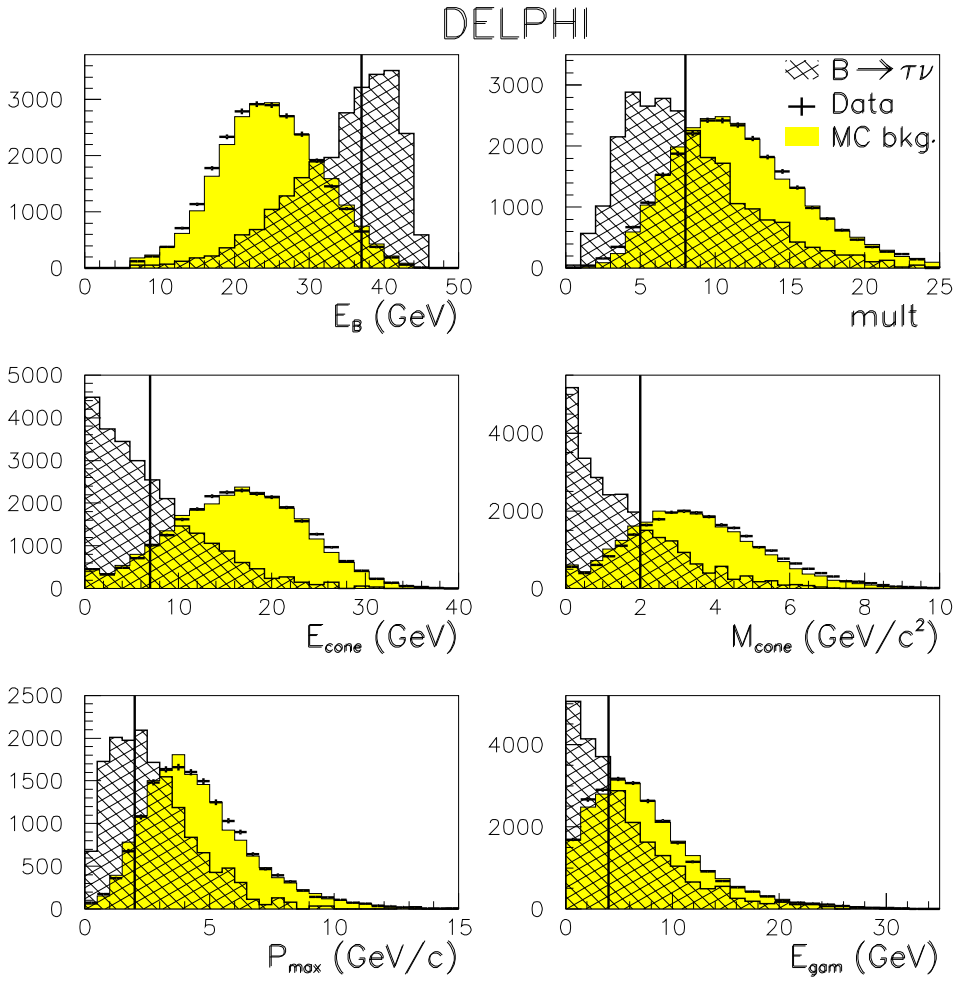

Figure 2: For the hadronic decay channel of the τ, simulated $B^- \to \tau^- \bar{\nu}_\tau$ signal (hatched) and background (shaded) distributions of the B meson energy, the hemisphere charged particle multiplicity, the total energy of particles inside the cone, the invariant mass of particles inside the cone, the maximum momentum of primary particles and the electromagnetic energy in the cone (see Section 3.2). Measured distributions in data (crosses) have been superimposed after having normalized the distributions from the simulation to the same integrated luminosity. Distributions for signal events have been normalized, in an arbitrary way, to the same number of events in the histogram. The vertical line defines the values of the cuts (see Section 3.2).

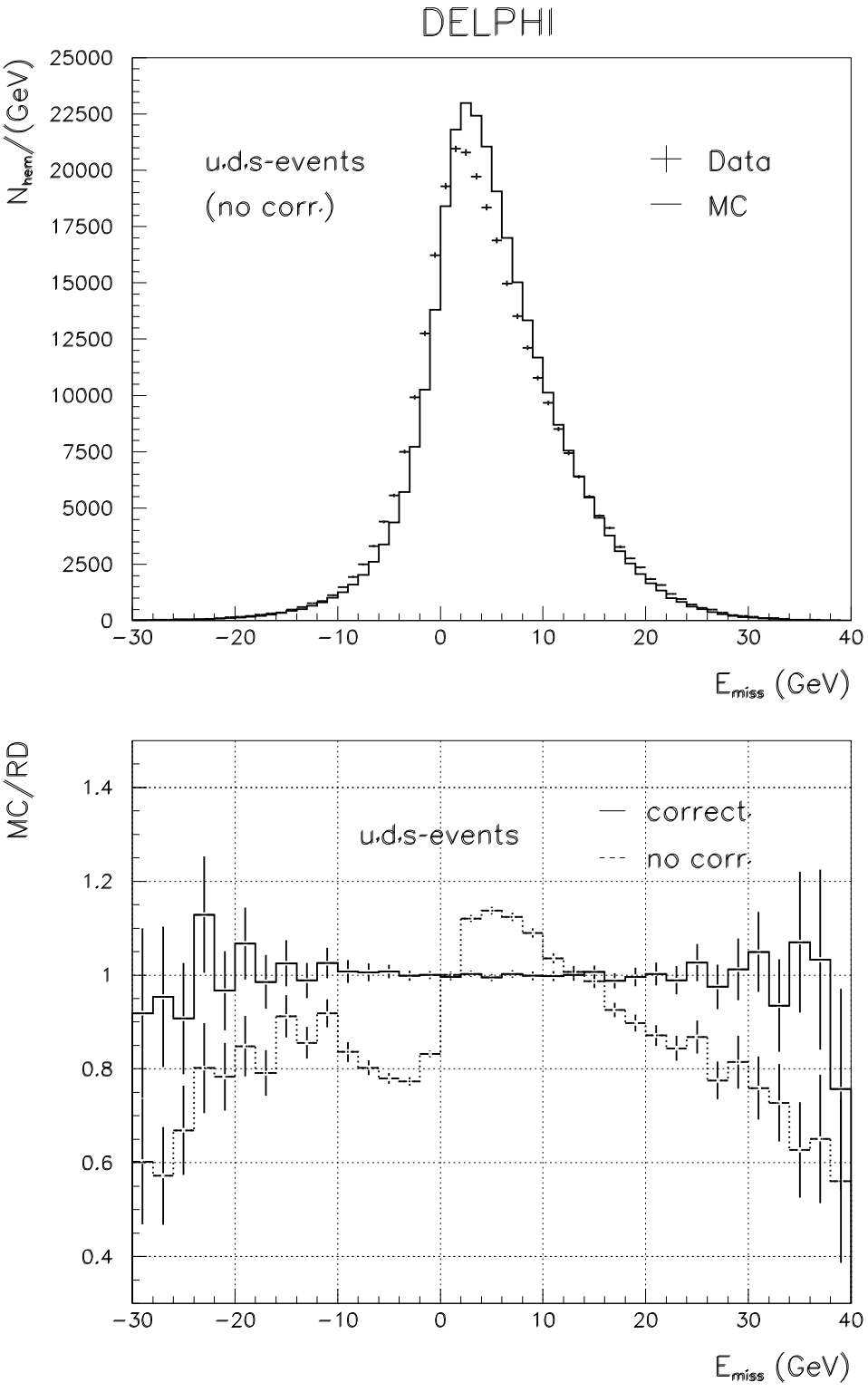

Figure 3: Comparison between real and simulated data of the missing energy distribution in each event hemisphere. The upper plots give these distributions for event samples depleted in heavy flavours decays. In the lower plots, the ratio between the two previous distributions are shown, before and after having applied the corrections detailed in Section 4.1.

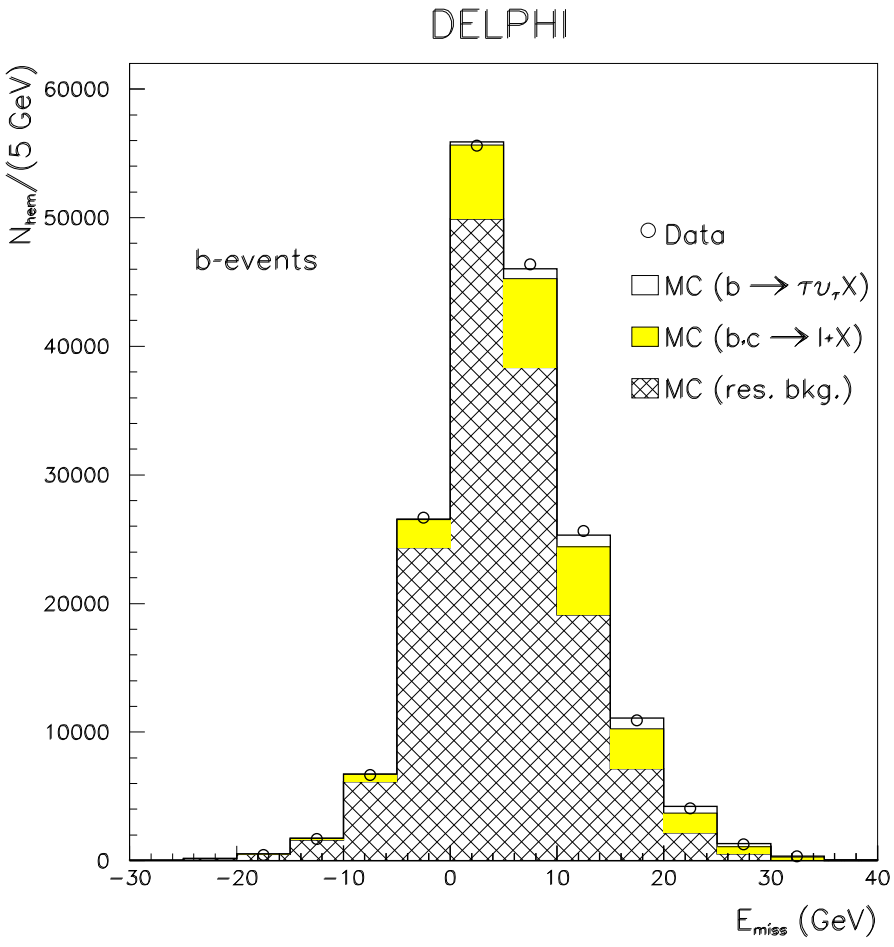

Figure 4: Hemisphere missing energy distributions for real data (circles) and simulation (histograms). The Monte Carlo events have been subdivided into the simulated $b \to \tau\bar{\nu}_\tau X$ signal, the semileptonic background and the residual background.

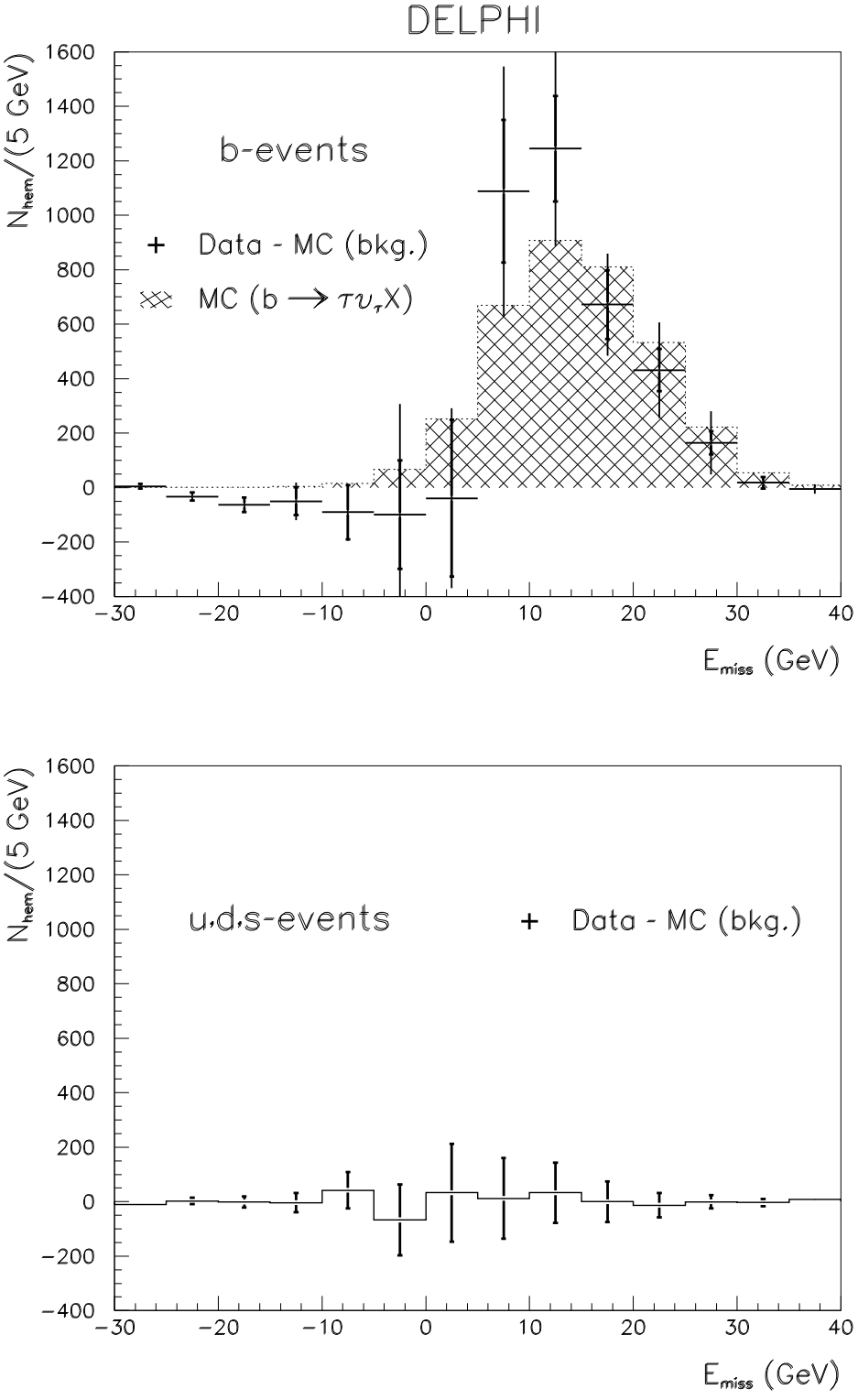

Figure 5: Difference of hemisphere missing energy distributions between real data and background simulation for both $b\bar{b}$ and light quark pairs enriched samples. The clear excess of data in the b sample is compared with the predicted missing energy spectrum of the $b \to \tau\bar{\nu}_\tau X$ signal (hatched area). The total error bars of the upper plot are computed from the quadratic sum of the statistical and systematic errors. The statistical errors of the data are presented by the thick error bars. The data and Monte Carlo histograms are normalized to the same number of entries in the missing energy range from -5 to 30 GeV.

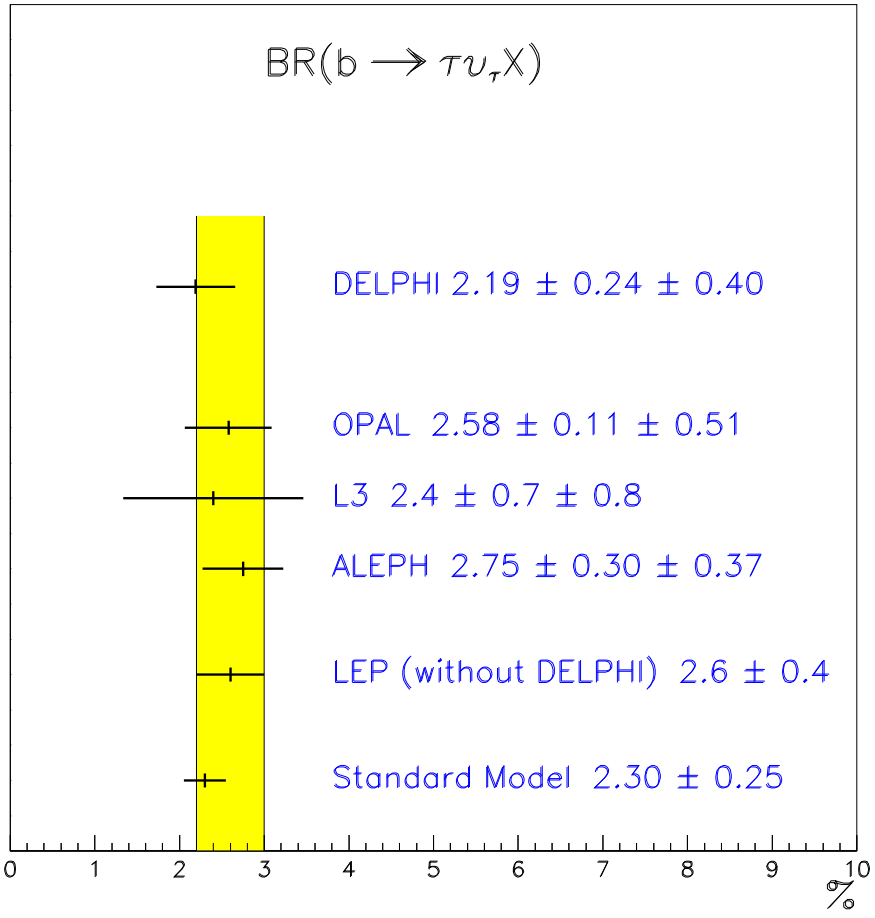

Figure 6: Comparison between the Standard Model prediction and experimental measurements of the $b \to \tau\bar{\nu}_\tau X$ branching fraction. All numbers are given in (%).

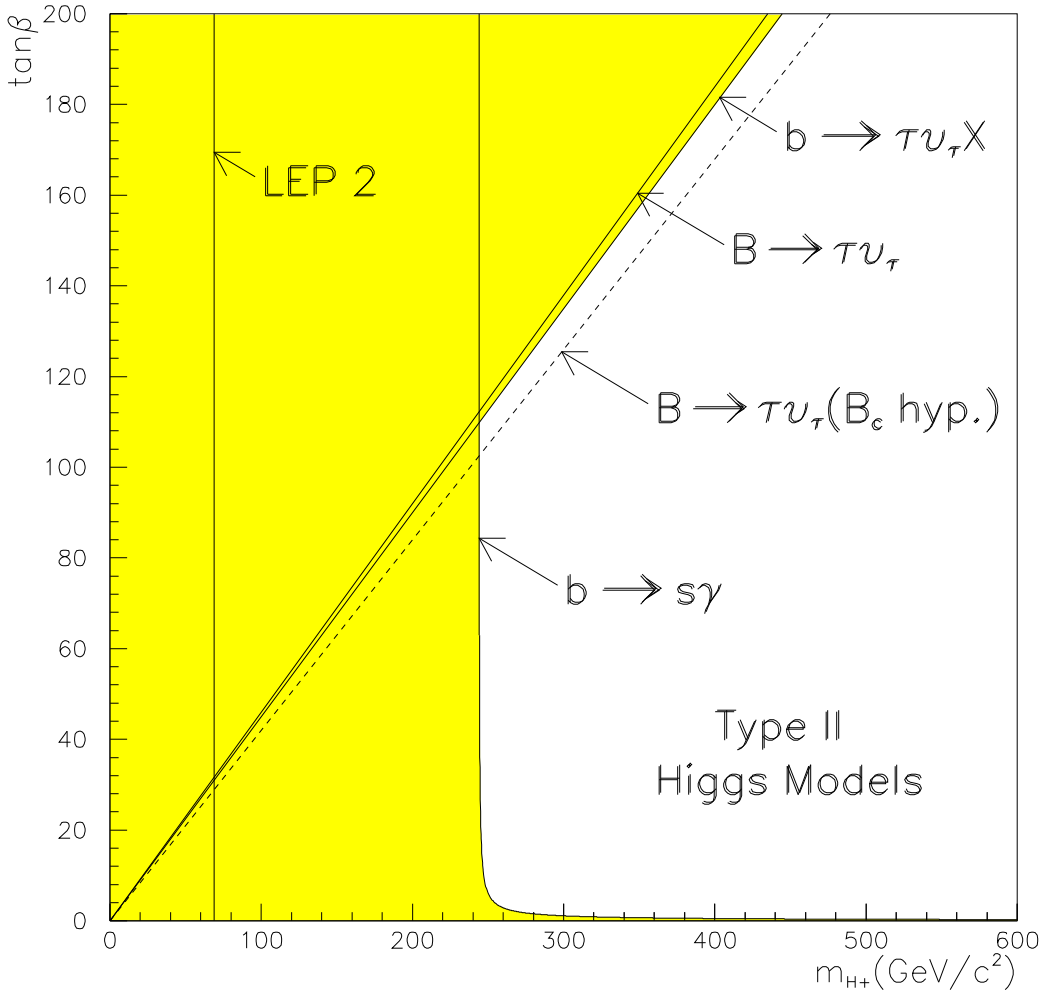

Figure 7: Limits on parameters of Type II Higgs doublet models extracted from the results of both inclusive and exclusive analyses, together with the constraints derived from the direct search of charged Higgs boson at LEP ($M_{H^\pm} > 69$ GeV/c^2 [25]) and the measurements of $b \to s\gamma$ [26]. The dotted line shows how the limit could improve using the B_c contribution hypothesis [7]. Shaded regions have been excluded at the 90% confidence level.